Journal of Cultural Heritage 61 (2023) 100–108

Contents lists available at ScienceDirect

Journal of Cultural Heritage

journal homepage: www.elsevier.com/locate/culher

VSI: LACONA XIII

UV femtosecond laser cleaning of encrusted historical stained-glasses

Evan Maina Maingi[a,b,c], María Pilar Alonso[a], Germán F. de la Fuente[b], Stéphan Dubernet[c], Yannick Lefrais[c], Rémy Chapoulie[c], Elodie Vally[d], Luis A. Angurel[b,*]

[a] Área de Historia del Arte, Departamento de Historia, Geografía y Comunicación, Universidad de Burgos, Pº Comendadores S/N, Spain & Unidad Asociada de I+D+i al CSIC "VIMPAC" 09001 Burgos Spain
[b] Instituto de Nanociencia y Materiales de Aragón (CSIC-University of Zaragoza), María de Luna 3, 50018 Zaragoza, Spain
[c] Archéosciences Bordeaux UMR 6034, CNRS, Bordeaux Montaigne University, France
[d] Maison Lorin, 46 rue de la Tannerie, 28000 Chartres, France

ARTICLE INFO

Article history:
Received 7 October 2022
Accepted 1 March 2023
Available online 3 April 2023

Keywords:
Conservation
Cultural heritage
Stained-glass
Ultra-short pulse lasers
Laser cleaning

ABSTRACT

Laser irradiation enables the removal of unwanted surface deposits from different materials in a safe and controllable manner. Laser parameters should be carefully selected to achieve the removal of the target contaminants without inducing damage to the substrate. Ultra-short pulse lasers have opened new opportunities for safe and controlled decontamination of cultural heritage materials because the thickness of material that is affected by the laser is limited. In this study, an ultraviolet femtosecond pulsed laser was used for the removal of unwanted encrustation formed on the surface of an historical colourless stained-glass sample from the Cuenca Cathedral in Spain. One of the sides of this glass exhibits a reddish-brown grisaille that also has to be preserved. A laser cleaning process has been designed to avoid heat accumulation while controlling the thickness of ablated material. In this context, a multi-step process was selected in order to be able to eliminate, in a controlled way, the crust layer without damaging the grisaille layer, or the glass substrate. In this case, laser irradiation in beam scanning mode with a pulse repetition frequency of 10 kHz proved to be effective for the safe cleaning of the glass. The latter was analysed before and after laser cleaning by optical and confocal microscopy, scanning electron microscopy, energy dispersive X-ray spectroscopy, X-ray fluorescence, and Raman spectroscopy, confirming that the crust layer was effectively eliminated without damaging the surface.

1. Introduction

Light is a fundamental element of the Gothic temples and the stained-glass windows allow light to flood its naves and chapels, transforming the entire space with their rich colours [1]. Humidity and temperature variations, dust, soot, acidic pollution, and microorganism attack, all have an impact on the deterioration process of glass materials and formation of strongly adhered encrustations. Ion-exchange processes promote corrosion on sensitive glasses, resulting in the creation of a gel layer and a crust of corrosion products on the glass surface. Furthermore, previous restoration interventions may affect the glass surface conditions, particularly when using harsh chemical cleaning methods or applying organic coatings that may further deteriorate the glass in a short- or long-term period [2–4].

Various cleaning methods have been applied for the removal of these encrustations, the most common being the combination of mechanical and chemical techniques. However, these conventional methods have several limitations. For instance, these processes have shown a possibility of causing long term damage to the glass surface or to the grisaille [5,6]. Other alternatives have to be explored in order to offer better options that would guarantee long term protection of a material after the restoration. One of these alternatives is the use of lasers as a cleaning tool in cultural heritage [7–13].

In the following decades, research on the applicability of laser technology as a cleaning tool has been increasing. At this moment, cleaning protocols using low frequency ns pulsed lasers have been stablished as a tool for cultural heritage restoration problems. Laser cleaning has also been applied in glass-based materials, and, in particular, on historical stained-glass windows [8-11,14-21].

* Corresponding author.
E-mail address: angurel@unizar.es (L.A. Angurel).

https://doi.org/10.1016/j.culher.2023.03.005

Laser technology has evolved very fast and ultra-short pulsed lasers (picosecond and femtosecond) are now available, opening new possibilities for precise and safer laser cleaning of cultural heritage objects. Pulse durations can now be adjusted within the ps and fs range, with pulse repetition frequencies ranging from a few kHz to MHz. The use of lasers with ultrashort pulse durations decreases heat accumulation on the irradiated surface and allows for more precise control of the laser affected material thickness [8,22-25].

Several mechanisms are involved in laser cleaning processes. They include thermal ablation, stress vibration, thermal expansion, evaporation, phase explosion, evaporation pressure, plasma shock [26]. The particular mechanism that is activated in a given problem depends on the laser system and the physical properties of the dirt material to be removed and those of the substrate. Reducing the pulse duration to values lower than 10 ps also triggers alternative laser-material interaction mechanisms, as for instance, the Coulomb explosion [27]. Moreover, a clear-cut definition of an ultra-short pulse was proposed by Gamaly [28] in relation to laser pulses with duration shorter than the major relaxation time for electron-to-lattice energy transfer, heat conduction and hydrodynamic expansion (typically with values lower than 100 fs). The latter considerations point to the fact that the present work includes a mixture of interaction mechanisms where the pulse repetition rate may play a relevant role when considering potential damage to the irradiated substrate.

The damage threshold is the minimal energy density required to generate a modification in the surface material. This modification may include material ablation, as well as physico-chemical modifications which may take into account, for instance, a change in colour or crack generation. When the material to be removed has a lower damage threshold than the original substrate, it is possible to define a self-limiting cleaning process because it does not affect the substrate [21].

A previous study [8] explored the interaction of ultra-short pulsed lasers (picosecond and femtosecond) with contemporary stained-glass samples frequently used in restoration interventions. The objective of this study was to advance the understanding of the phenomena that take place during laser cleaning of glass materials, as well as to establish the influence of different laser parameters that may enable the definition of a safe cleaning protocol. This work also explored the potential application of ultra-short pulsed lasers (picosecond IR and fs IR) for cleaning historical colourless stained-glass, based on cleaning protocols that were established using contemporary glasses. Following this study, it was evident that the applied IR laser radiation was able to safely and efficiently remove the brown-coloured outmost layer of the unwanted crust covering the glass. This efficiency was found to decrease significantly when the laser subsequently irradiated the inner whiter layers that appear following external layer removal.

2. Research aim

In order to overcome the ineffectiveness of Nd:YAG fundamental wavelength on whitish stratification, the possible use of UV radiation was considered. This paper thus explores and presents the applicability and efficiency of UV laser irradiation towards the removal of a gypsum-like encrustation layer formed on the surface of an historical colourless stained-glass.

The objective of the applied methodology is to develop a safer laser cleaning protocol. It is based on the development of a multi scan approach with levels of energy low enough to avoid any damage when the crust layer is removed and the laser reaches the grisaille or the glass surface. The developed laser cleaning treatment has been designed to control the amount of crust layer that is eliminated in each scan, offering the possibility of not completely removing the crust layer if it is required. Optical micrography, SEM, and Raman analysis were used to evaluate the changes induced on the sample surface during laser cleaning.

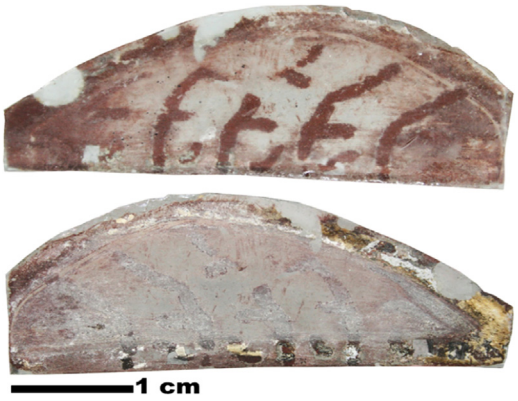

Fig. 1. Photographs of the colourless stained-glass sample from the Cuenca Cathedral: recto (upper photograph) and verso (lower photograph).

3. Materials and methods

3.1. Historical stained-glass sample

The Cuenca Cathedral is one of the earliest Gothic cathedrals in Spain. The historic centre of Cuenca was listed as a UNESCO World Heritage Site in 1996, with the cathedral of Santa María of Cuenca being the iconic monument. The construction of the Cathedral began in the late 12th century, after the conquest of the city of Cuenca by Alfonso VIII, and it was largely completed around the second half of the 13th century [29]. A colourless historical stained-glass sample measuring 4.8 cm x 2 cm x 2 mm was selected for this study (Fig. 1). Due to the documentary sources and the presence of this piece among the remains of decontextualized stained-glass windows make it is difficult to determine the provenance and dating. Thus, the exact chronology cannot be specified, but it is related to the context of the stained-glass activity in the cathedral during the 15th century. The glass has a reddish-brown grisaille that appears to have been applied in striated patterns that could have been part of a larger iconography. This grisaille layer was well adhered to the bulk glass. The glass exhibited a significant amount of crust on its surface that had accumulated due to exposure to different environmental conditions over the centuries. The surface corrosion crust was spread mostly on the painted layer with the thinnest crust forming on the glass surface itself. This glass piece had remnants of yellow-coloured putty on one of the edges, as can be observed on the right side of the bottom photograph in Fig. 1.

3.2. Experimental

3.2.1. Laser system

Laser treatments were carried out using a femtosecond (fs) laser (Carbide model, Light Conversion, Vilnius, Lithuania), also coupled to a galvanometric mirror system (Direct Machining Control, UAB, Vilnius, Lithuania). Laser irradiation was performed using UV emission at an output wavelength of 343 nm. This laser can emit with three wavelengths. Emission in the UV was selected because the surface absorption layer is thinner and after an analysis of the optical response of selected modern stained-glass samples with different colours, differences in absorption between different glasses were found minimal for UV, when compared with equivalent visible and IR laser irradiation [30]. The maximum laser output power available was 11 W and the treatments were performed

with a pulse duration of 238 fs. At the working distance, the beam exhibited an elliptical shape with axes $2a$=41 µm and $2b$=29 µm, using the $1/e^2$ criterium [31].

In order to ensure that thermal gradients were kept below safe values, laser cleaning was performed using a frequency of 10 kHz [8]. Cleaning treatments were performed using a beam scanning configuration in which the laser scans the sample surface at a given speed, v_L=150 mm/s, resulting in a distance of 15 µm between consecutive pulses. This is the maximum distance between pulses that produces sufficient overlap to generate a uniform energy distribution along the laser beam scan line [32]. A similar distance between subsequent beam scan lines (δ_{lin}=15 μm) was also selected. To control the amount of removed material, low values of energy per pulse (E_{pulse}) were selected and the scan process was repeated several times.

3.2.2. Surface characterization

The glass surface was observed before and after the laser treatment with a JSM 6360-LV Scanning Electron Microscope (SEM). Images were taken in a vacuum mode at 20 Pa. A piece of a polished transverse sample of this glass was also analysed using a Field Emission Scanning Electron Microscope (FE-SEM, Carl Zeiss MERLIN). The glass surface was also observed without coating using low electron acceleration voltages, ca. 3 kV. Semi quantitative elemental analysis of the glass composition was performed using Energy Dispersive X-ray Spectroscopy (EDS, INCA350, Oxford Instruments) with acquisition times up to 500 s. The observations were also complemented using a portable loop microscope and a ZEISS SteREO Discovery.V8 (8:1 manual zoom range) microscope to optically assess the morphological features and the degree of degradation of the glass. General morphological aspects were documented and evaluated by photography under standard reflected light using a Canon EOS 400D digital camera.

The topography of the glass surface before and after laser cleaning was also measured using a confocal microscope (Sensofar PLμ2300).

X-ray maps to determine the elemental chemical composition distribution over the glass surface and the grisaille were acquired at voltages of 15 kV and 40 kV, respectively, with a current of 1000 μA, a collimator measuring 0.5 × 0.5 mm^2, and frame accumulation counts set at 5.

Raman spectroscopy was also used for molecular and structural investigation before and after laser cleaning. The equipment used in this work was a Renishaw type RM2000. Under laser focusing, the spatial resolution can be estimated at 2 × 2µm^2 at the surface (perpendicular to the optical axis, XY) and around 3 µm in depth (Z). All the spectra were acquired with a 532 nm laser, a grating at 1800 gr/mm and a spectrometer entrance slit of 50 µm, ensuring a satisfactory spectral resolution. Each spectrum was obtained by an accumulation (summation) of several consecutive acquisitions. These acquisitions are a fixed combination between attenuation of the laser power and time per point. The latter is systematically adapted so that the most intense spectral component does not exceed the saturation of the detector (approximately 120,000 cts) without degradation of the point under the laser beam.

4. Results and discussion

4.1. Analysis of the historical glass before laser cleaning

Before any laser cleaning intervention, an in-depth understanding of the structure and composition of the stained-glass, the grisaille, and the corrosion crust is essential for defining and conceiving a laser cleaning procedure that will guarantee effective and safe decontamination of the glass.

Table 1 shows the composition of the glass obtained by EDS analysis. These values are the average of six measurements obtained in areas of approximately 100 × 25 μm^2 distributed in the cross section of the sample. The glass contains 63.9% wt SiO_2, 11.5% wt CaO, 7.5% wt K_2O and 8.5% wt Na_2O. The composition of this historical glass includes a significant amount of K_2O, confirming that it is a soda-potash-lime silica glass with similar content of soda and potash. The presence of additional oxides was also confirmed, such as a network forming Al_2O_3 (4.2% wt), and a network stabilizer MgO (4.6% wt). The presence of this relatively high amount of Al_2O_3 may be justified by its effect on viscosity and surface tension, which are both enhanced by the addition of aluminium compounds to the glass network. In addition, it improves the glass resistance to thermal shock [33].

Figure 2(a) shows the cross-section of the grisaille layer. It has a thickness that ranges between 45 and 75 µm. As it can be observed in the supplementary material (Figure S1), the layer contains different components and exhibits high porosity. Elemental analysis of the different phases is presented in Table 2. They show that grisaille consists of a matrix (region 1) of lead silica glass, as the glass phase, and iron oxide (Fe_2O_3) as the pigment. Region 2 corresponds to a grain of iron oxide, while region 5 shows iron oxide particles with higher porosity. In addition, aluminium and potassium-aluminium silicates are detected.

Another important issue is the good chemical compatibility and the good adherence between the grisaille and the glass, where a diffusion layer of approximately 750 nm in thickness is observed (Figure S1). This type of microstructure shows that during the production of the grisaille, the ideal temperature to allow the grisaille to adhere to the glass was reached (roughly 600–750 °C) [34].

The complete glass surface is covered by a white crust layer. As deduced from Fig. 2(b) and suggested from the data in Table 2, this layer is not uniform. SEM analysis shows that the morphology of the grains that form this layer is different depending on the analysed region. On top of the glass (Figure 2(b)), regular submicrometric particles are observed. By contrast, on top of the grisaille (Supplementary Figure S2) crust grains are larger and with irregular shapes. EDS analyses also show that different regions exhibit different chemical compositions. In one case, the composition included an important amount of S, while in the other case, the crust exhibited a relatively rich concentration of Ca and Mg which could infer the presence of calcite ($Ca_2(CO_3)_2$) or calcium magnesium carbonate ($CaMg(CO_3)_2$) and the initial formation of anhydrite ($CaSO_4$) or gypsum ($CaSO_4{\cdot}2H_2O$). In other regions, P was also detected, suggesting the presence of phosphates.

The above analyses were complemented with Raman spectroscopy studies to obtain local structural information on both, crystalline and amorphous phases, providing excellent spatial resolution. Fig. 3 and Supplementary Figure S3 collect the different types of spectra that have been obtained in specific areas of interest within the stained-glass sample that are indicated in Figure S4. In particular, Figure S3 shows two Raman spectra that were obtained on the white crust growth regions directly over the glass surface and mainly correspond to carbon-based compounds, associated with organic residues present on the sample surface. They have been observed for different types of materials, such as soot, lamp black, carbon black or bistre [35–37] and exhibit a band at about 1582 ± 5 cm^{-1}, known as the G (ordered C) band, and another peak at 1340 ± 12 cm^{-1}, known as the D (disordered C) band [35]. Moreover, broad bands at ca. 617 ± 7 cm^{-1} and at 1085 ± 5 cm^{-1}, associated with the glass surface, are also detected, indicating that on top of the glass, the crust layer is thinner.

Fig. 3 shows some spectra that were recorded in regions where the white crust was on top of the grisaille. In addition to the carbon-base compounds, the Raman analysis further revealed a heterogeneous corrosion product composed of hydrated and

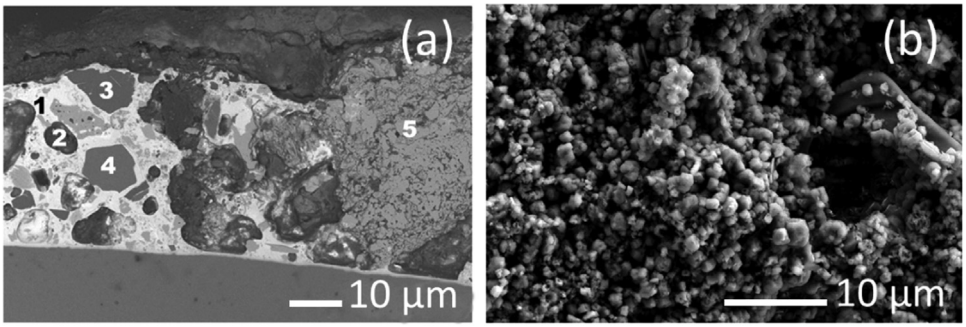

Fig. 2. (a) Cross-section on the region with grisaille. (b) Micrograph of the surface of the crust layer observed on top of the glass.

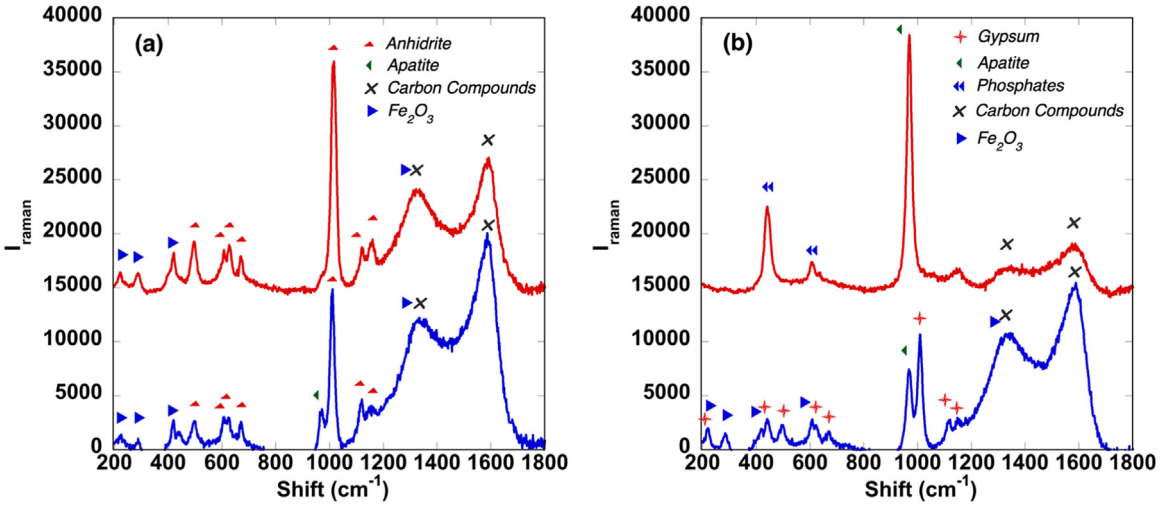

Fig. 3. Raman spectra in different regions of the surface of the sample where white crust appears on top of the grisaille. Some spectra have been shifted along the Y-axis for clarity. Exact positions are presented in Supplementary material, Figure S4.

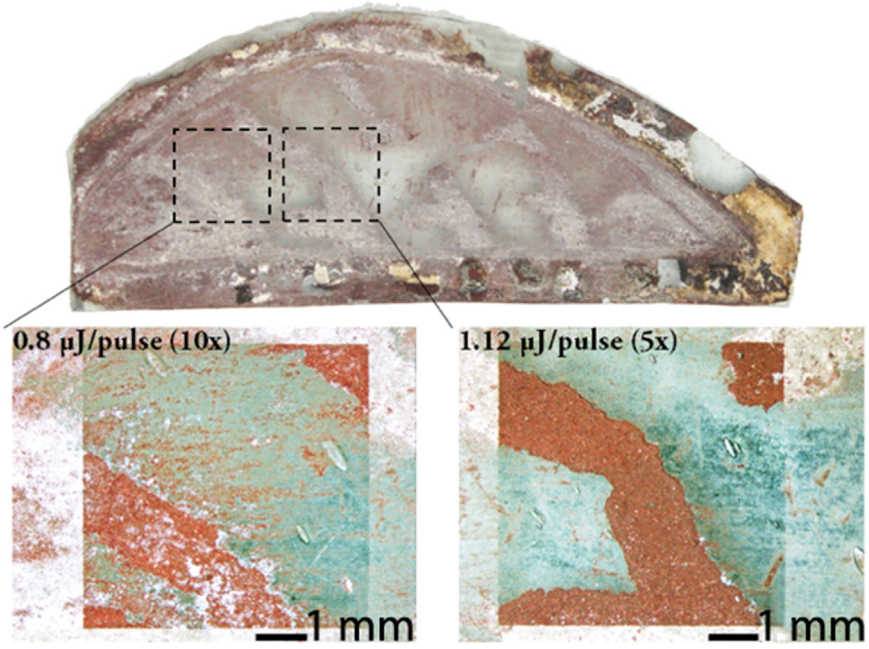

Fig. 4. Optical micrographs of two regions that were cleaned using (left) 10 scans with E_{pulse}=0.8 µJ/pulse and (right) 5 scans with E_{pulse}=1.12 µJ/pulse.

Table 1
Elemental composition (%at) determined by EDS on the glass and% wt of the main oxides.

% at	O	Si	Ca	Na	K	Al	Mg	Cl	Fe
	57.9	*23.4*	*4.5*	*6.0*	*3.5*	*1.8*	*2.5*	*0.4*	*0.1*
% wt	SiO_2	CaO	Na_2O	K_2O	Al_2O_3	MgO			
	63.9	*11.5*	*8.5*	*7.5*	*4.2*	*4.6*			

Table 2
Main oxides (% wt) on the different regions of the grisaille indicated in Fig. 2 and elemental composition (% at) determined by EDS in different regions of the crust layer.

%wt	SiO_2	CaO	Na_2O	K_2O	Al_2O_3	MgO	Fe_2O_3	PbO			
Grisaille (1)	*27.4*	*1.3*	*1.0*	–	*0.9*	*0.6*	*4,3*	*64,5*			
Grisaille (2)	–	–	–	–	–	–	*100*	–			
Grisaille (3)	*87.3*	–	–	*3.3*	*8.8*	*0.6*	–	–			
Grisaille (4)	*59.4*	–	–	*18.4*	*22.2*	–	–	–			
Grisaille (5)	–	–	–	–	–	–	*100*	–			
Grisaille (Interface)	*39.9*	*4.0*	*0.9*	*1.6*	*1.3*	*1.9*	*4.4*	*39.9*			
%at	**O**	**Si**	**Ca**	**Na**	**K**	**Al**	**Mg**	**Fe**	**Pb**	**P**	**S**
Crust (1)	*74.1*	*6.6*	–	*0.9*	–	*3.0*	*1.2*	*2.5*	*2.8*	–	*8.7*
Crust (2)	*75.8*	*0.9*	*12.4*	–	–	*0.3*	*10.4*	–	–	–	*0.2*
Crust (3)	*71.8*	*13.8*	–	*1.2*	–	*3.9*	*1.8*	*4.4*	*0.8*	*1.1*	–

anhydrous sulphates, as well as the presence of apatite. Figure 3(a) shows some Raman spectra where the main contribution is associated to the presence of anhydrite, with the characteristic SO_4 symmetric stretching mode at 1015 cm^{-1}. The symmetric bending and asymmetric stretching modes of SO_4 tetrahedra appear in two bands i.e. one at 420 cm^{-1} and 496 cm^{-1} and the other one at 1122 cm^{-1} and 1159 cm^{-1}. The bands observed at 628 cm^{-1} and 671 cm^{-1} are attributed to its asymmetric bending vibration mode [38]. Additionally, the weak intensity band at 608 cm^{-1} originates, according to Liu et al. [39], in the asymmetric bending mode of SO_4.

In addition, Raman analysis helped identify the presence of apatite as part of the crust covering the colourless glass surface. The typical single band of apatite appears at 970 cm^{-1} in Figure 3(a) and 3(b), consistent with previous measurements reported in the literature [40]. Bands associated with the presence of Fe_2O_3 are also identified in Figure 3(a).

Finally, Figure 3(b) also confirms the detection of gypsum in other regions of the sample. In this case, the most intense band in the Raman spectrum is observed at 1010 cm^{-1} and is assigned to the symmetric stretch vibration mode of the SO_4 tetrahedra. The presence of gypsum is also confirmed with the appearance of the double symmetric bending bands at ca. 441 cm^{-1} and 497 cm^{-1}. Bands assigned to the asymmetric bending vibration modes of sulphates appear at about 608 cm^{-1} and 670 cm^{-1}, and the maxima observed at 1118 cm^{-1} and 1152 cm^{-1} are assigned to their asymmetric stretching modes. Since the Raman spectra were acquired in the 200–2000 cm^{-1}spectral range, the characteristic bands for the stretching vibration modes of water in gypsum could not be confirmed. These bands have previously been reported by White [38] and Bhagavantam [41] as appearing at 3406 cm^{-1} and 3494 cm^{-1}.

An additional band corresponding to PO_4 symmetric bending appears at ca. 441 cm^{-1}, while its asymmetric bending mode band can be observed at about 608 cm^{-1}.

4.2. Surface crust removal with the UV fs laser system

Initial laser treatments were applied in areas of 6 × 6 mm^2 targeting the white crust covering both the glass and the brown grisaille layer, with the laser processing parameters indicated in Section 3.2.1. The effectiveness of the treatment was checked by combining the energy of each pulse and the number of scans performed during the cleaning process. The laser scan direction was rotated 90° for each subsequent scan.

The objective of these initial treatments was to check the performance of the selected laser parameters and to make a prior assessment of any damage that may be induced on the glass and the grisaille. The laser irradiation was applied gradually increasing the energy per pulse while carefully monitoring any colour or physical changes on the surface of the glass. Single line scans carried out in modern stained-glass samples have enabled establishing damage thresholds at or above 0.4 J/cm^2. This value is reduced to 0.15 J/cm^2 when similar scans to those performed in this work are applied in 1 × 1 mm^2 areas. At each power level, the laser irradiation was applied during a number of scans i.e. from one to about ten times or until crust removal was detected. Once glass or grisaille started to appear on the surface, the laser treatment was stopped. Examples of two different regions that were treated with 10 laser scans applying an E_{pulse}=0.80 μJ/pulse (0.09 J/cm^2, 360 GW/cm^2) and five scans with E_{pulse}=1.12 μJ/pulse (0.12 J/cm^2, 485 GW/cm^2) are presented in Fig. 4. The cleaning process using E_{pulse}=0.8 μJ/pulse was not enough to completely remove the crust layer. After having applied 10 scans the crust was not completely eliminated. This result shows the very fine control of the cleaning process, which facilitates the maintenance of a thin layer of crust material when necessary by establishing a specific number of scans.

By increasing the energy to 1.12 μJ/pulse the crust layer could be completely removed. Thus, at this power level, five laser irradiation scans proved to be sufficient to completely remove the crust from the surface minimising the damage to the glass substrate, or to the grisaille. Figure S5 shows the aspect of the surface in another region where a treatment with 7 scans and E_{pulse}=1.12 μJ/pulse was applied. In this case, the laser cleaning treatment was carried out on both sides. Figures S5(a) and S5(b) show the effect on the side containing grisaille, while Figures S5(c) and S5(d) show the result on the opposite side. The opposite side of this glass was not covered with any grisaille and had a thin crust layer evenly and smoothly spread out on the surface. The images presented in Figure S5 demonstrate that the above cleaning parameters are effective on both sides of the stained glass. Confocal topographies recorded in the limit of the cleaned region (Supplementary Figure S6) show that the height of the step that is observed in the limit between the cleaned area and the original one is ca. 28 μm.

It was already established that E_{pulse}=1.12 μJ/pulse was safe for both, the glass substrate and the grisaille. In order to evaluate the reproducibility of these results, alternative areas with different dimensions were selected for laser cleaning using the same E_{pulse} level. The selected regions are presented in Fig. 5(a). In region I,

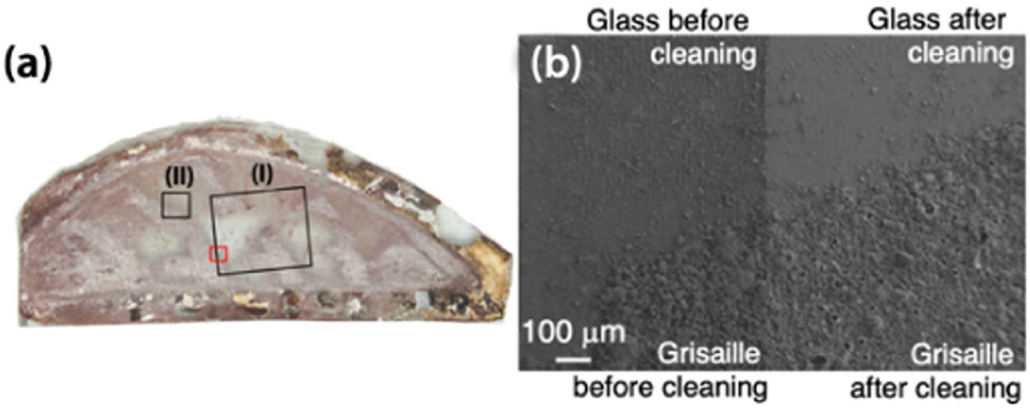

Fig. 5. (a) Areas selected for laser cleaning with the fs UV laser. The treatment began with the area on the right (I) followed by that in the centre (II). (b) SEM micrograph showing the border between cleaned and non-cleaned regions in the position indicated by the small red square.

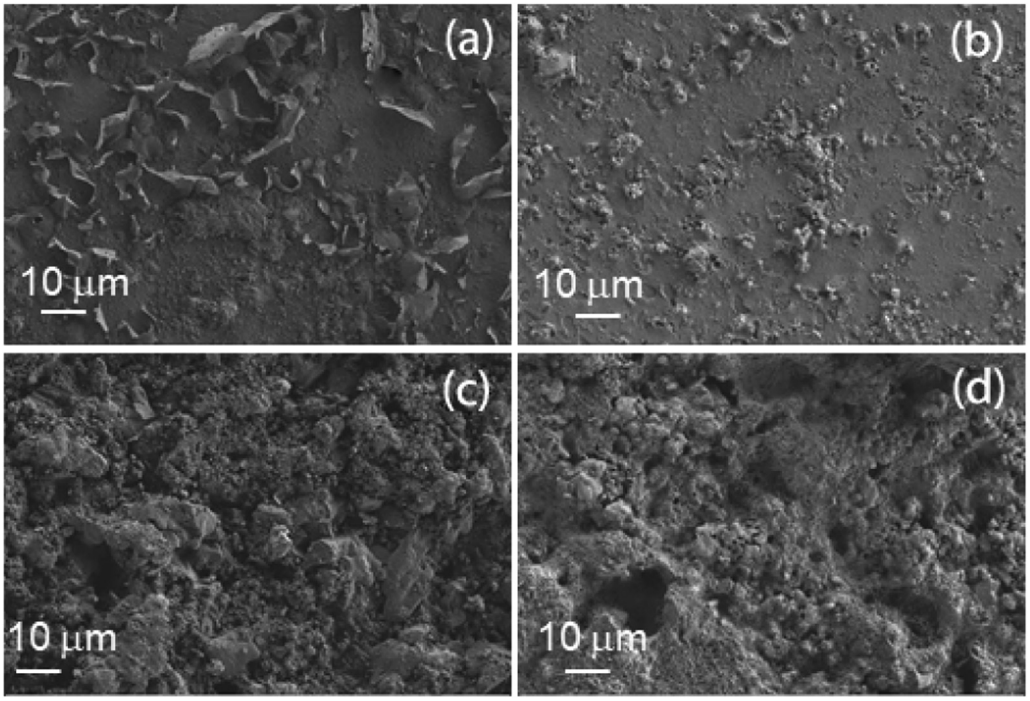

Fig. 6. SEM micrograph of treatment from area I. (a) Glass surface with a thin grisaille layer before cleaning. (b) Similar surface after cleaning. (c) Grisaille surface before cleaning. (d) Grisaille surface after cleaning.

corresponding to a 1 × 1 cm^2, the cleaning protocol was repeated 7 times; in region II, however, for a 2 × 2 mm^2 area, the process was repeated only 5 times.

Fig. 5(b) shows a micrograph of the border of region I, in the position indicated with a red square in Fig. 5(a). The left part of the image shows the aspect of the surface before applying the laser cleaning treatment using 7 scans with E_{pulse}=1.2 μJ/pulse. The right part of the image shows its aspect after eliminating the crust layer. The upper part of the figure exhibits a region of the sample where a very thin layer of grisaille was present on the glass surface. In the bottom part of the image, a region with a thicker grisaille layer is observed. Fig. 6 shows details of the different regions. In some areas, a crust layer with a laminar structure has been observed (Fig. 6(a)). After having applied the cleaning protocol (Fig. 6(b)), the surface is not damaged and even the thin pigment layer was not affected. When the laser is applied on top of the grisaille, the surface maintains its topography, and no significant differences are observed between the sample surface before (Fig. 6(c)) and after laser treatment (Fig. 6(d)).

A similar laser cleaning treatment was also applied on area II. In this case, only 5 series were applied. Although the treatment did not satisfactorily remove all the crust layer in some areas, Fig. 7 shows that these cleaning conditions were sufficient to have an efficiently cleaned section maintaining the integrity of the original sample in most of the area. The unwanted white crust was efficiently removed without inducing any melt or change of colour in the underlying paint layer. This is also observed in Fig. 7(b). The two yellow lines indicate two borders of the laser treated area. SEM micrographs presented in the supplementary material (Fig. S7) show the aspect of the crust layer above the grisaille before laser irradiation, a region that is denser than in the corresponding region presented in Fig. 6(c), and the resultant aspect after laser cleaning. It is clear that no melting is induced on the grisaille surface. Combining these observations with the colour observed in

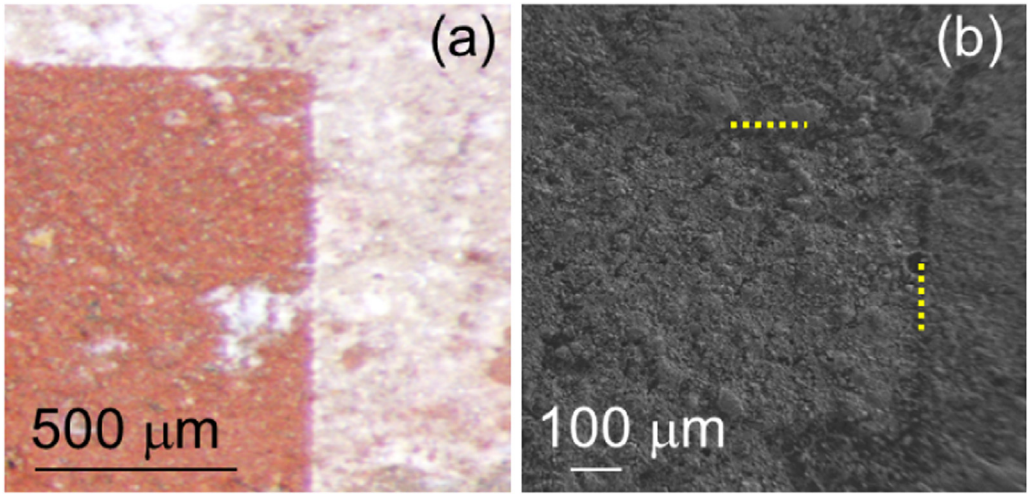

Fig. 7. (a) Optical micrograph of area II after laser cleaning with 5 series using 1.12 μJ/pulse. (b) FESEM micrograph showing the aspect of the surface before and after laser irradiation. The two lines help to identify the horizontal and vertical limits between cleaned and original regions.

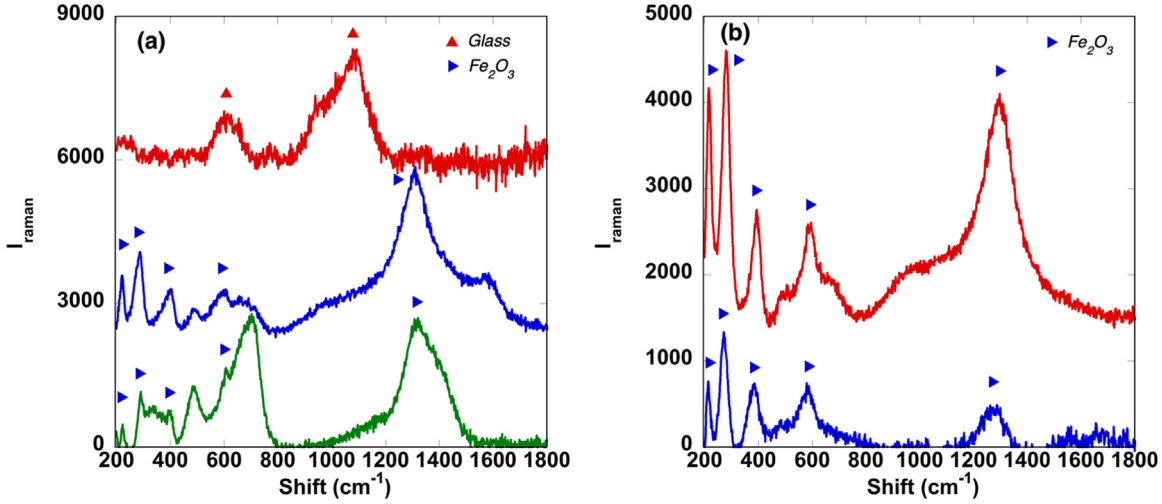

Fig. 8. Raman spectra in two cleaned regions of the colourless glass. Exact positions are presented in Supplementary material, Fig. S3. Red spectrum in (a) was measured on the glass, the other four spectra were recorded on different positions on top of the grisaille.

Fig. 7(a), it is possible to assume that pigment is not damaged during laser treatment.

EDS analysis performed on the laser cleaned region shows a great reduction of the characteristic elements of the different compounds that are present in the crust, mainly S, Ca and P. This has also been confirmed with Raman analysis, as shown in Fig. 8, where Raman spectra measured in two different regions after laser cleaning are given. It is important to remark on the differences between these spectra and those recorded in regions that were not cleaned (Fig. 3). The first difference is that the Raman intensity is very low in these spectra in comparison with those measured in similar regions before cleaning. The second one is that these spectra show that the crust has been completely removed because the peaks associated with anhydrite, gypsum, calcite and carbon compounds have disappeared (Table 3). Images in the supplementary material (Fig. S4) show the areas that were analysed and the particular points are indicated with circles of the same colours corresponding to those used in the spectra (Fig. 8). In the first region, the red spectrum was measured in an area without grisaille, while the blue and green ones were recorded in the area with grisaille. The spectrum obtained on the glass exhibits a characteristic band at 1083 cm^{-1} and a second one at 611 cm^{-1}. In the other four positions on top of the grisaille, the trends are different. They now exhibit an intense band in the 1290–1310 cm^{-1} region, as well as other bands in the 200–600 cm^{-1} region that are mainly associated to Fe_2O_3. Optical micrography, SEM and Raman analysis, and the comparison with the same analysis performed on the original glass, confirm that the developed laser cleaning treatment is effective to eliminate the crust layer without affecting neither the glass nor the grisaille.

The determination of the elements present in the different regions of the sample was also performed by XRF mapping. The maps were obtained from an area of the glass sample with dimensions 23 × 13 mm^2 with a central region that was cleaned with the laser. Results are presented in the supplementary material, Fig. S8 and Table 4 indicates the evolution of the different elements that were analysed. S, P and Ca maps confirm a reduction of the relative amount of these elements in the laser cleaned region. Simultaneously, the measured increase in Si and K confirms that the laser cleaning process is effective in removing the crust layer and that the glass surface can thus be reached during the measurement. In the case of Al and Mn, XRF spectra show that these elements are uniformly distributed within the glass sample, thus only a slight increase can be detected in the laser cleaned areas. XRF

Table 3
Comparison of Raman bands observed in the original surfaces and after having applied the laser cleaning protocols. In the case of the anhydrite, gypsum and calcite, the main peaks are indicated in bold.

	Anhidrite	*Gypsum*	*Calcite*	*Apatite*	*Phosphates*	*Carbon Comp.*	*Fe_2O_3*	*Glass*
Bands	*393*	*209*	*280*	*970*	*441*	*1340*	*222*	*611*
	499	*415*	*710*		*608*	*1582*	*297*	*1083*
	609	*492*	***1086***				*410*	
	626	*617*	*1437*				*613*	
	674	***1008***					*662*	
	1017	*1141*					*1320*	
	1129							
	1277							
	1319							
BEFORE CLEANING								
Fig. 3(a) Red sp.	*X*					*X*	*X*	
Fig. 3(a) Blue sp.	*X*			*X*		*X*	*X*	
Fig. 3(b) Red sp.				*X*	*X*	*X*		
Fig. 3(b) Red sp.		*X*		*X*		*X*	*X*	
Fig. S3						*X*		*X*
AFTER CLEANING								
Fig. 8(a) Red sp.								*X*
Fig. 8(a) Blue sp.							*X*	
Fig. 8(a) Green sp.							*X*	
Fig. 8(b) Red sp.							*X*	
Fig. 8(b) Blue sp.							*X*	

Table 4
Comparison of the amount of each element in the area that has been cleaned: ↑ = Increase, ↓ = Decrease, ≈↑ =Moderate increase.

Element	Si	Ca	K	Al	Mn	S	P	Fe	Pb
Variation	↑	↓	↑	≈↑	≈↑	↓	↓	↑	↑

spectra of Pb and Fe suggest that their detection is important for the identification of areas covered by grisaille. The concentrations of these elements increase upon laser cleaning, confirming that the laser process eliminates the upper contaminant layer without deteriorating the original grisaille.

5. Conclusions

The results presented in this work confirm that fs lasers pave the way for developing respectful laser cleaning protocols, in particular for the restoration of materials with very low thermal conductivity, as historical stained-glass samples. The use of UV radiation limits the crust layer thickness that is affected during irradiation. A multi scan process, with low E_{pulse} values, was applied in this study in order to exert precise control over the amount of crust layer removed during each laser irradiation scan. Heat accumulation was controlled by combining the above process with laser pulse repetition frequency values in the 10 kHz range. The obtained results confirm that thin contaminant crust layers can be safely removed over grisaille layers and the glass substrate, while minimising the risk of their deterioration.

Acknowledgements

This work was supported by H2020-MSCA-ITN-EJD/ED-ARCHMAT action under the Marie Sklodowska-Curie grant agreement no. 766311. Partial support is obtained from Gobierno de Aragón (research group T54_20R). The use of Servicio General de Apoyo a la Investigación at the University of Zaragoza is acknowledged. This work has been performed in the framework of the Unidad Asociada de I+D+I al CSIC "Vidrio y Materiales del Patrimonio Cultural (VIMPAC)", by INMA (CSIC-University of Zaragoza) and University of Burgos.

Supplementary materials

Supplementary material associated with this article can be found, in the online version, at doi:10.1016/j.culher.2023.03.005.

References

[1] L. Lara Martínez, Palabras de cristal: las vidrieras contemporáneas de la Catedral de Cuenca, Comunicación y Hombre 10 (2014) 121–130, doi:10.32466/eufv-cyh.2014.10.165.121-130.
[2] F. Becherini, A. Bernardi, A. Daneo, F.G. Bianchini, C. Nicola, M. Verità, Thermal stress as a possible cause of paintwork loss in medieval stained glass windows, Stud. Conserv. 53 (2014) 238–251, doi:10.1179/sic.2008.53.4.238.
[3] R.H. Brill, Crizzling – a problem in glass conservation, Stud. Conserv. 20 (1975) 121–134, doi:10.1179/sic.1975.s1.021.
[4] S. Fearn, D.S. McPhail, V. Oakley, R.H. Brill, Room temperature corrosion of museum glass: an investigation using low-energy SIMS, Stud. Conserv. 231–232 (2004) 121–134, doi:10.1179/sic.1975.s1.021.
[5] R. Abd-Allah, Chemical cleaning of soiled deposits and encrustations on archaeological glass: a diagnostic and practical study, J. Cult. Herit. 14 (2013) 97–108, doi:10.1016/j.culher.2012.03.010.
[6] C. Altavilla, E. Ciliberto, S.La Delfa, S. Panarello, A. Scandurra, The cleaning of early glasses: investigation about the reactivity of different chemical treatments on the surface of ancient glasses, Appl. Phys. A: Mater. Sci. Process. 92 (2008) 251–255, doi:10.1007/s00339-008-4499-x.
[7] C. Fotakis, D. Anglos, V. Zafiropulos, S. Georgiou, V. Tornari, Lasers in the Preservation of Cultural Heritage: Principles and Applications (2006) ISBN 10: 0750308737.
[8] E.M. Maingi, M.P. Alonso, L.A. Angurel, M.A. Rahman, R. Chapoulie, S. Dubernet, G.F. de la Fuente, Historical stained-glass window laser preservation: the heat accumulation challenge, Boletín de La Sociedad Española de Cerámica y Vidrio 61 (2022) S69–S82, doi:10.1016/j.bsecv.2021.12.003.
[9] H. Römich, K. Dickmann, P. Mottner, J. Hildenhagen, E. Müller, Laser cleaning of stained glass windows - Final results of a research project, J. Cult. Herit. 4 (2003) 112–117, doi:10.1016/s1296-2074(02)01187-1.
[10] H. Römich, P. Mottner, J. Hildenhagen, K. Dickmann, G. Hettinger, F. Bornschein, Comparison of Cleaning Methods for Stained Glass Windows, in: K. Dickmann,

C. Fotakis, J.F. Asmus (Eds.), Lasers in the Conservation of Artworks. Springer Proceedings in Physics, Springer, Berlin, Heidelberg, 2005 vol 100, doi:10.1007/3-540-27176-7_20.
[11] Ed. by R. Salimbeni, R. Pini, S. Siano, M. Vannin, A. Corallini, Excimer laser cleaning of stained glass samples, in: W. Kautek, E. Konig (Eds.), LACONA I: Lasers in the Conservation of Artworks, Restauratorenblätter Sonderband, Verlag Mayer & Comp, Wien, Austria, 1995, pp. 83–88. Ed. by1997ISBN: 3-901025-68-5.
[12] S. Siano, J. Agresti, I. Cacciari, D. Ciofini, M. Mascalchi, I. Osticioli, A.A. Mencaglia, Laser cleaning in conservation of stone, metal, and painted artifacts: state of the art and new insights on the use of the Nd:YAG lasers, Appl. Phys. A: Mater. Sci. Process. 106 (2012) 419–446, doi:10.1007/s00339-011-6690-8.
[13] M. Sokhan, P. Gaspar, D.S. McPhail, A. Cummings, L. Cornish, D. Pullen, F. Hartog, C. Hubbard, V. Oakley, J.F. Merkel, Initial results on laser cleaning at the Victoria & Albert Museum, natural history museum and tate gallery, J. Cult. Herit. 4 (2003) 230–236, doi:10.1016/s1296-2074(02)01219-0.
[14] G.M. Bilmes, J. Vallejo, C. Costa-Vera, M.E. Garcia, High efficiencies for laser cleaning of glassware irradiated from the back: application to glassware historical objects, Appl. Phys. A 124 (2018) 347, doi:10.1007/s00339-018-1761-8.
[15] U. Drewello, R. Weißmann, S. Rölleke, E. Müller, S. Wuertz, F. Fekrsanati, C. Troll, R. Drewello, Biogenic surface layers on historical window glass and the effect of excimer laser cleaning, J. Cult. Herit. 1 (2000) 161–171, doi:10.1016/S1296-2074(00)00183-7.
[16] F. Fekrsanati, J. Hildenhagen, K. Dickmann, C. Troll, U. Drewello, C. Olaineck, UV-laser radiation: basic research of the potential for cleaning stained glass, J. Cult. Herit. 1 (2000) 155–160, doi:10.1016/S1296-2074(00)00150-3.
[17] F. Fekrsanati, S. Klein, J. Hildenhagen, K. Dickmann, Y. Marakis, A. Manousaki, V. Zafiropulos, Investigations regarding the behaviour of historic glass and its surface layers towards different wavelengths applied for laser cleaning, J. Cult. Herit. 2 (2001) 253–258, doi:10.1016/S1296-2074(01)01130-X.
[18] A.M. Joyce, D.M. Kane, Comparison of front and back laser irradiation in laser cleaning of silica particles from silica glass, in: PICALO 2006 - 2nd Pacific International Conference on Applications of Laser and Optics - Conference Proceedings, 299, 2006, pp. 299–304, doi:10.2351/1.5056947.
[19] Y.F. Lu, S. Komuro, Y. Aoyagi, Laser-induced removal of fingerprints from glass and quartz surfaces, Jpn. J. Appl. Phys. 33 (1994) 4691–4696, doi:10.1143/JJAP.33.4691.
[20] H. Römich, A. Weinmann, Laser cleaning of stained glass windows. Overview on an interdisciplinary project, J. Cult. Herit. 1 (2000) 151–154, doi:10.1016/S1296-2074(00)00186-2.
[21] F. Fekrsanati, J. Hildenhagen, K. Dickmann, P. Mottner, U. Drewello, Feasibility studies on applying UV-lasers for the removal of superficial depositis from historic glass, Stud. Conserv. 46 (2001) 196–210, doi:10.2307/1506810.
[22] C. Kerse, H. Kalaycloğ Lu, P. Elahi, B. Çetin, D.K. Kesim, Ö. Akçaalan, S. Yavaş, M.D. Aşlk, B. Öktem, H. Hoogland, R. Holzwarth, F. Ö. Ilday, Ablation-cooled material removal with ultrafast bursts of pulses, Nature 537 (2016) 84–88, doi:10.1038/nature18619.
[23] R. Weber, T. Graf, P. Berger, V. Onuseit, M. Wiedenmann, C. Freitag, A. Feuer, Heat accumulation during pulsed laser materials processing, Opt. Express 22 (2014) 11312, doi:10.1364/oe.22.011312.
[24] H. Zhang, S.M. Eaton, J. Li, P.R. Herman, Heat accumulation during high repetition rate ultrafast laser interaction: waveguide writing in borosilicate glass, J. Phys. Conf. Ser. 59 (2007) 682–686, doi:10.1088/1742-6596/59/1/144.
[25] A. Md Rahman, G.F. de la Fuente, J.M. Carretero, E.M. Maingi, M.P. Alonso, R. Alonso Alcalde, R. Chapoulie, N. Schiavon, L.A. Angurel, Sub-ns-pulsed laser cleaning of an archaeological bone from the Sierra de Atapuerca, Spain: a case study, SN Appl. Sci. 3 (2021) 865, doi:10.1007/s42452-021-04850-8.
[26] G. Zhu, Z. Xu, Y. Jin, X. Chen, L. Yang, J. Xu, D. Shan, Y. Chen, B. Guo, Mechanism and application of laser cleaning: a review, Opt. Lasers Eng. 157 (2022) 107130, doi:10.1016/j.optlaseng.2022.107130.
[27] R. Stoian, D. Ashkenasi, A. Rosenfeld, E.E.B. Campbell, Coulomb explosion in ultrashort pulsed laser abation of Al_2O_3, Phys. Rev. B 62 (2000) 13167–13173, doi:10.1103/PhysRevB.62.13167.
[28] E.G. Gamaly, The physics of ultra-short laser interaction with solids at non-relativistic intensities, Phys. Rep. 508 (2011) 91–243, doi:10.1016/j.physrep.2011.07.002.
[29] E. Torrero, D. Sanz, M.N. Arroyo, V. Navarro, The cathedral of Santa María (Cuenca, Spain): principal stone characterization and conservation status, Int. J. Conserv. Sci. 6 (2015) 625–632.
[30] E.M. Maingi, Laser-based Intervention in Historical Stained-Glasses PhD Thesis, University of Burgos and University Bordeaux Montaigne, 2022.
[31] J.M. Liu, Simple technique for measurements of pulsed Gaussian-beam spot sizes, Opt. Lett. 7 (1982) 196, doi:10.1364/ol.7.000196.
[32] L. Porta-Velilla, N. Turan, Á. Cubero, W. Shao, H. Li, G.F. de la Fuente, E. Martínez, Á. Larrea, M. Castro, H. Koralay, S. Cavdar, J. Bonse, Highly regular hexagonally-arranged nanostructures on Ni-W alloy tapes upor irradiation with untrashort UV laser pulses, Nanomaterials 12 (2022) 2380, doi:10.3390/nano12142380.
[33] A.M.C. Pinto, T.A.B.C. Sanjad, R.S. Angélica, M.L. Da Costa, R.S. Paiva, T. Palomar, 19th century stained-glass windows from Belém do Pará (Brazil): analytical characterisation and pathology, Boletín de la Sociedad Española de Cerámica y Vidrio 57 (2018) 133–141, doi:10.1016/j.bsecv.2017.10.005.
[34] P. Fernandes, M. Vilarigues, L.C. Alves, R.C. da Silva, Stained glasses from Monastery of Batalha: non-destructive characterisation of glasses and glass paintings, J. Cult. Herit. 9 (2008) 5–9, doi:10.1016/j.culher.2008.07.005.
[35] E.P. Tomasini, B. Gómez, E.B. Halac, M. Reinoso, E.J. Di Liscia, G. Siracusano, M.S. Maier, Identification of carbon-based black pigments in four South American polychrome wooden sculptures by Raman microscopy, Herit. Sci. 3 (2015) 4–11, doi:10.1186/s40494-015-0049-y.
[36] G. Marucci, A. Beeby, A.W. Parker, C.E. Nicholson, Raman spectroscopic library of medieval pigments collected with five different wavelengths for investigation of illuminated manuscripts, Anal. Methods 10 (2018) 1219–1236, doi:10.1039/c8ay00016f.
[37] A. Sadezky, H. Muckenhuber, H. Grothe, R. Niessner, U. Pöschl, Raman microspectroscopy of soot and related carbonaceous materials: spectral analysis and structural information, Carbon 43 (2005) 1731–1742, doi:10.1016/j.carbon.2005.02.018.
[38] S.N. White, Laser Raman spectroscopy as a technique for identification of seafloor hydrothermal and cold seep minerals, Chem. Geol. 259 (2009) 240–252, doi:10.1016/j.chemgeo.2008.11.008.
[39] Y. Liu, Raman, MIR, and NIR spectroscopy study of calcium sulfates: gypsum, bassanite, and anhydrite, in: 40th Lunar and Planetary Science Conference, 50, 2009, p. 2128.
[40] K.D. Litasov, N.M. Podgornykh, Raman spectroscopy of various phosphate minerals and occurrence of tuite in the Elga IIE iron meteorite, J. Raman Spectrosc. 48 (2017) 1518–1527, doi:10.1002/jrs.5119.
[41] S. Bhagavantam, Interpretation of Raman spectra in crystals: anhydrite and gypsum, in: Proceedings of the Indian Academy of Sciences - Section A, 8, 1938, pp. 345–348, doi:10.1007/BF03045904.